744 *Macromolecules* **2011**, *44*, 744–750
DOI: 10.1021/ma102858b

Macromolecules
ARTICLE

# Poly(ionic liquid) Latexes Prepared by Dispersion Polymerization of Ionic Liquid Monomers

**Jiayin Yuan* and Markus Antonietti**

*Max-Planck-Institute of Colloids and Interfaces, Department of Colloid Chemistry, Research Campus Golm, Am Muehlenberg 1, D-14476 Golm, Germany*

*Received December 15, 2010; Revised Manuscript Received January 11, 2011*

ABSTRACT: In this contribution, we report the facile preparation of vinylimidazolium-typed poly(ionic liquid) (PIL) latexes and nanoparticles via dispersion polymerization of ionic liquid monomers in aqueous solutions. A homologous series of vinylimidazolium-typed ionic liquid monomers with different alkyl tail length (C8−C18) were synthesized via quaternization of 1-vinylimidazole with corresponding *n*-alkyl bromides. Dispersion polymerization of these monomers was conducted at a monomer concentration of 50 g/L in aqueous solution at 70 °C without addition of further stabilizers. For ionic liquid monomers with sufficiently long alkyl chains (≥C12), PILs nanoparticles of 20−40 nm in diameter were found, which were self-stabilizing in aqueous media. In the same procedure, preparation of cross-linked PIL nanoparticles was performed in the presence of 10 mol % of divinylimidazolium-based cross-linker. The as-synthesized cross-linked PIL nanoparticles could be transferred into organic solvents, such as polar DMF, and nonpolar toluene after anion exchange with lithium bis(trifluoromethylsulfonyl)imide. This dispersion polymerization requires no dispersing agent and potentially enables a large scale synthesis of PIL nanoparticles in both aqueous and organic solutions. The application spectrum of this unique type of organic nanoparticles is expectedly broad; e.g., the particles are useful as powerful binders and dispersants for coatings and as colloidal templates.

## Introduction

Ionic liquids (ILs) are composed of an organic cation (imidazolium, pyridinium, tetraalkylammonium, etc.) and an anion such as halide, tetrafluoroborate, hexafluorophosphate, triflate, amidotriflate, dicyanamide, etc. Despite the ionic chemical structure, it is the characteristic feature that ILs exhibit low melting point below 100 °C. They have been widely studied for nearly one century because of their unique properties including superior ionic conductivity, high polarity, large heat capacity, strong solubilizing ability, excellent thermal and chemical stability, and so forth.[1−8]

Polymeric or polymerized ILs (PILs) refer to a special type of polyelectrolytes which carry an IL species in each of the repeating units. Benefiting from the intensive studies on ILs in the past decades, recently PILs have stirred steadily expanding interest in the fields of polymer chemistry and materials science, not only because of the combination of the unique properties of ILs with the macromolecular architecture, but also a matter of creating new properties and functions. The rapid progress and explosive development in this field is reflected by the very large body of recent publications.[9−12] The major advantages of using a PIL instead of an IL are the enhanced mechanical stability, improved processability, durability, and spatial controllability over the IL species via macromolecular architecture. Their promising applications involve polymeric electrolytes, catalytic membranes, ionic conductive materials, carbon dioxide absorbents, microwave absorbing materials, stabilizing agent, and carbon precursors.[12−17]

PILs having imidazolium moiety in each repeating unit are the most studied ones.[18,19] In general, the three major polymer species are main chains of poly(meth)acrylate, polystyrene, and poly(1-vinylimidazolium).[20−24] They were dominantly prepared by conventional free radical polymerization of IL monomers (ILMs) due to the great tolerance of a radical polymerization toward impurities, moistures, and other active and functional groups. As a new approach, the preparation of PILs via controlled/"living" radical polymerizations have been very recently reported, which are expected to enable the precise design and control of macromolecular architecture of IL species on a meso-/nanoscale.[25−30] There are also other emerging polymerization techniques that have appeared for the preparation of PILs which have further pushed the limit of the potentialities of PILs.[31−34]

In this contribution, we demonstrate a facile method to prepare PIL latexes and nanoparticles via aqueous dispersion polymerization of vinylimidazolium-typed ionic liquid monomers (ILMs) at 70 °C without dispersant. With sufficiently long alkyl chains (≥C12), PILs nanoparticles of 20−40 nm in diameter formed. Cross-linked nanoparticles stable in aqueous as well as polar organic solvents, were obtained in the same procedure in the presence of 10 mol % of divinylimidazolium-based cross-linker. Anion exchange with bis(trifluoromethylsulfonyl)imide anion produced stable nanoparticle dispersion in nonpolar solvents, such as toluene. The sensitivity of PIL nanoparticles toward ionic strength was quantitatively demonstrated by monitoring the size evolution of nanoparticles in dependence of salt concentration. This preparation method of PIL nanoparticles requires no dispersant agent and potentially can be scaled up. It is worth noting that the synthesis of PIL nanoparticles has been seldom reported, and their charming application as stabilizing agents and binders was demonstrated very recently.[24,35,36] To our best knowledge, this is the first report of stable PIL nanoparticles by dispersion polymerization.

*Corresponding author. E-mail: jiayin.yuan@mpikg.mpg.de.

 Published on Web 01/31/2011 

## Experimental Section

**Materials.** 1-Vinylimidazole (Aldrich 99%), 1-bromooctane (Aldrich 99%), 1-bromodecane (Aldrich 98%), 1-bromododecane (Aldrich 98%), 1-bromotetradecane (Aldrich 97%), 1-bromohexadecane (Aldrich 97%), 1-bromooctadecane (Aldrich 98%), 1,4-dibromobutane (Aldrich 99%), water-soluble nonionic azo initiator VA86 (Wake Chemicals), ionic initiator 2,2′-azobis(2-methylpropionamidine) dihydrochloride (V50, Aldrich 97%), and lithium bis(trifluoromethylsulfonyl)imide (Aldrich 97%) were used as received without further purifications. All solvents used were of analytic grade.

**Preparation of Ionic Liquid Monomers.** A general synthetic protocol for ionic liquid monomers (ILMs) was as follows: 0.1 mol of 1-vinylimidazole, 0.1 mol of *n*-alkyl bromide and 30 mL of methanol were loaded into a 100 mL reactor. The mixture was stirred at 60 °C for 15 h. After cooling down, the reaction mixture was added dropwise into 1 L of diethyl ether. The white precipitate was filtered off and dried at room temperature until constant weight. In the case of 1-bromooctane, a yellow liquid was obtained instead of a white powder. 1,4-butanediyl-3,3′-bis-l-vinylimidazolium dibromide (BVD) as divinylimidazolium cross-linking agent was prepared in the same manner except that the molar ratio of 1-vinylimidazole to 1,4-dibromobutane was 2:1 in the reaction.

*3-n-Octyl-1-vinylimidazolium Bromide* (*ILM-8, Viscous Liquid at Room Temperature*). $^1$H NMR (DMSO-$d_6$, $\delta$, ppm): 10.02 (1H), 8.42 (1H), 8.12 (1H), 7.41 (1H), 6.09 (1H), 5.38 (1H), 4.27 (2H), 1.82 (2H), 1.19 (10H), 0.78 (3H). $^{13}$C NMR (DMSO-$d_6$, $\delta$, ppm): 135.74, 129.23, 123.74, 119.78, 109.08, 49.63, 31.62, 29.67, 28.94, 28.83, 25.97, 22.50, 14.31.

*3-n-Decyl-1-vinylimidazolium Bromide* (*ILM-10, Sludgy at Room Temperature*). $^1$H NMR (DMSO-$d_6$, $\delta$, ppm): 10.00 (1H), 8.41 (1H), 8.11 (1H), 7.42 (1H), 6.09 (1H), 5.39 (1H), 4.27 (2H), 1.82 (2H), 1.18 (14H), 0.79 (3H). $^{13}$C NMR (DMSO-$d_6$, $\delta$, ppm): 135.74, 129.24, 123.74, 119.76, 109.05, 49.62, 31.75, 29.68, 29.39, 29.32, 29.15, 28.90, 25.98, 22.55, 14.33.

*3-n-Dodecyl-1-vinylimidazolium bromide* (*ILM-12, Mp = 47 °C*). $^1$H NMR (DMSO-$d_6$, $\delta$ ppm): 9.92 (1H), 8.37 (1H), 8.08 (1H), 7.40 (1H), 6.07 (1H), 5.40 (1H), 4.25 (2H), 1.82 (2H), 1.20 (18H), 0.81 (3H). $^{13}$C NMR (DMSO-$d_6$, $\delta$, ppm): 135.77, 129.29, 123.74, 119.74, 109.05, 49.63, 31.78, 29.66, 29.53, 29.51, 29.46, 29.33, 29.21, 28.91, 26.00, 22.57, 14.35.

*3-n-Tetradecyl-1-vinylimidazolium Bromide* (*ILM-14, Mp = 62 °C*). $^1$H NMR (DMSO-$d_6$, $\delta$, ppm): 9.89 (1H), 8.35 (1H), 8.06 (1H), 7.39 (1H), 6.06 (1H), 5.40 (1H), 4.25 (2H), 1.82 (2H), 1.20 (22H), 0.82 (3H). $^{13}$C NMR (DMSO-$d_6$, $\delta$, ppm): 135.77, 129.31, 123.73, 119.71, 109.05, 49.64, 31.77, 29.63, 29.55 (overlapped peaks), 29.50, 29.45, 29.31, 29.18, 28.90, 25.99, 22.55, 14.34.

*3-n-Hexadecyl-1-vinylimidazolium Bromide* (*ILM-16, Mp = 69 °C*). $^1$H NMR (DMSO-$d_6$, $\delta$, ppm): 9.83 (1H), 8.33 (1H), 8.04 (1H), 7.38 (1H), 6.04 (1H), 5.41 (1H), 4.24 (2H), 1.82 (2H), 1.21 (26H), 0.83 (3H). $^{13}$C NMR (DMSO-$d_6$, $\delta$, ppm): 135.77, 129.31, 123.73, 119.69, 109.03, 49.62, 31.79, 29.64, 29.56 (overlapped peaks), 29.52, 29.48, 29.34, 29.21, 28.92, 26.00, 22.57, 14.33.

*3-n-Octadecyl-1-vinylimidazolium Bromide* (*ILM-18, Mp = 78 °C*). $^1$H NMR (DMSO-$d_6$, $\delta$, ppm): 9.87 (1H), 8.34 (1H), 8.05 (1H), 7.39 (1H), 6.05 (1H), 5.36 (1H), 4.25 (2H), 1.81 (2H), 1.21 (30H), 0.82 (3H). $^{13}$C NMR (DMSO-$d_6$, $\delta$, ppm): 135.79, 129.33, 123.74, 119.71, 109.07, 49.65, 31.81, 29.66, 29.58 (overlapped peaks), 29.54, 29.52, 29.38, 29.23, 28.95, 26.04, 22.59, 14.35.

*1,4-Butanediyl-3,3′-bis-l-vinylimidazolium Dibromide* (*BVD, Mp = 150 °C*). $^1$H NMR (DMSO-$d_6$, $\delta$, ppm): 9.52 (2H), 8.30 (2H), 8.02 (2H), 7.42 (2H), 6.00 (2H), 5.42 (2H), 4.28 (4H), 1.86 (4H). $^{13}$C NMR (DMSO-$d_6$, $\delta$, ppm): 135.89, 129.30, 123.71, 119.75, 109.26, 48.81, 26.18.

**Polymerization Process.** All homopolymerizations were conducted in the following procedure. In a 250 mL Schlenk flask, 5 g of ILM, 150 mg of VA86, and 100 mL of water were mixed. The mixture was completely deoxygenated by three cycles of freeze−pump−thaw procedure and was backfilled with argon. The flask was then stirred in an oil bath thermostated at 70 °C for 24 h. After cooling down to room temperature, a portion of the reaction mixtures was freeze-dried for proton nuclear magnetic resonance ($^1$H NMR) measurements in $CDCl_3$ to determine the monomer conversion. Except ILM-8, the polymerizations of all other monomers reached a nearly full conversion (99−100%). In the case of the long-alkyl-chain (C12−C18) PILs, stable reaction solutions were obtained and exhaustively dialyzed against deionized water. In the case of the intermediate-alkyl-chain (C8 and C10) PILs, the upper suspension was separated and dialyzed against deionized water; the precipitate at the bottom was washed with deionized water several times and dried at 80 °C until constant weight.

To prepare the cross-linked PIL nanoparticles from ILM-C14, -C16, and -C18, the polymerization was carried out in the same procedure, except 10 mol % (with regard to the ILMs used) of the cross-linker BVD was added. The nanoparticle dispersion in DMF was prepared by dialysis of aqueous nanoparticle solution against DMF or by direct addition of concentrated nanoparticle solution into an excess of DMF.

Anion exchange process was performed by adding excessive lithium bis(trifluoromethylsulfonyl)imide into an aqueous solution of nanoparticles. The solid precipitate was washed three times with methanol and then redispersed in toluene by ultrasonication and gentle heating.

For the study of solution behavior of PIL nanoparticles in the presence of external KBr salt, a KBr solution was added dropwise to a 10 g/L of aqueous nanoparticle solution under vigorous stirring. The size evolution of the nanoparticles at different KBr concentration was monitored by dynamic light scattering.

**Characterization Methods.** The average particle size (volume-weighted) was determined by dynamic light scattering (DLS) at 90° with a NICOMP particle sizer (model 370, NICOMP particle sizing systems, Santa Barbara, CA).

Transmission electron microscopy (TEM) was performed with a Zeiss EM 912 Omega microscope operating at 120 kV. The TEM samples were prepared by placing one drop of the diluted dispersion of PIL nanoparticles on a 200 mesh carbon-coated copper grid and left in air to dry.

Field emission scanning electron microscopy (FESEM) observations were performed on a LEO 1550-Gemini instrument. The samples were loaded on carbon coated stubs and coated by sputtering a Au/Pd alloy prior to imaging.

$^1$H and $^{13}$C nuclear magnetic resonance ($^1$H and $^{13}$C NMR) measurements were carried out at room temperature using a Bruker DPX-400 spectrometer operating at 400.1 MHz. DMSO-$d_6$ and $CDCl_3$ were used as solvents.

Differential scanning calorimetry (DSC) measurements were performed on a Perkin-Elmer DSC-1 instrument. The samples were first heated up to 100 °C, and then the samples were subjected to a cooling process from +100 to −50 °C at a cooling rate of 10 K/min. They were kept at −50 °C for 2 min. Finally, the samples were reheated to 100 °C at a heating rate of 10 K/min. The melting point of ionic liquid monomers was determined by the heating curve.

## 3. Results and Discussion

As early as in 1973, Salamone et al. first reported the preparation of several 3-*n*-alkyl-l-vinylimidazolium iodide ionic liquid monomers (ILMs), which in turn were homopolymerized into PILs in aqueous solution ($C_{monomer} \sim 100$ g/L) by free radical initiation.[21,37,38] They observed that the solution behavior of the as-synthesized polymers was directly related to the length scale of

**Scheme 1. Synthetic Route to Poly(ionic liquid) Latexes *via* Dispersion Polymerization of Ionic Liquid Monomers with or without Divinylimidazolium Cross-Linking Agent**

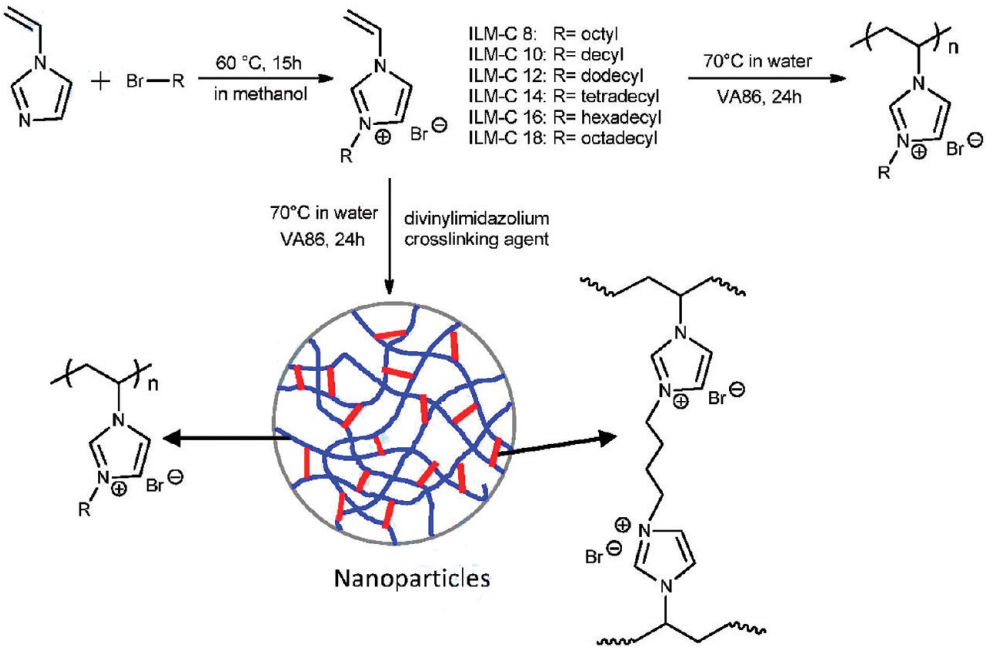


the alkyl chains. After the polymerization, the polymers were fairly water-soluble for short alkyl (methyl and propyl) chains and totally insoluble for the intermediate alkyl (hexyl and heptyl) chains; interestingly, for even longer alkyl (decyl and hexadecyl) chains, a stable dispersion together with 30 wt % of precipitate was obtained. Following this work, more and more attention was directed to the studies of radical polymerization of vinylimidazolium or vinylpyridinium-based ILMs with long alkyl tails.[35,39−44] However, these activities mainly focused on the physicochemical behaviors of PILs in aqueous media; it remains yet unclear when polymerized directly in aqueous media, what is the true morphology of the PIL structures, taking into account that these polymers when dried were no longer water-soluble. Our research interest here lies in the identification of possible PIL nanostructures in aqueous solution. PILs based on 3-ethyl-1-vinylimidazolium bromide and 3-*n*-butyl-1-vinylimidazolium bromide were molecularly dissolved in water, thus of no interest to us; 3-*n*-hexyl-1-vinylimidazolium bromide was excluded after first trials from this research as the polymerization produced completely insoluble polymers in water.

. In the monomer synthesis, the reaction proceeded in the absence of a radical stabilizer, nevertheless $^1$H NMR measurements pointed out that the monomers did not polymerize at all at these conditions and on the time scale of the synthetic procedure (15 h). The physical properties of ILMs were correlated with the alkyl chains, as also demonstrated by other groups before.[21,37,38,42,45] For example, at room temperature ILM-C8 is liquid and ILM-C10 is sludgy, while the others exist in a solid state with melting points above room temperature; ILM-C16 and ILM-C18 are only soluble in water assisted by gentle heating to overcome the crystalline state, while the others are fairly soluble in water at room temperature.

The dispersion polymerization of ILMs in aqueous solution was conducted at 70 °C for 24 h initiated by VA86 in the absence of any added dispersant (Scheme 1). ILM-16 was initially chosen as a model monomer at different concentrations of 25, 37.5, 50, 100, and 150 g/L to find out the suitable window of the monomer concentration. It was observed that at 100 and 150 g/L, precipitation took place during the polymerization; on the other hand, polymerizations conducted at 50 g/L or less provided a translucent stable solution. $^1$H NMR measurements showed the complete vanishing of the vinyl protons, indicating that the monomer conversion reached 100%. Accordingly, all dispersion polymerizations were carried out at a monomer concentration of 50 g/L in water. The results are summarized in Table 1 (entries 1−6).

It is clear from Table 1 that except ILM-C8 and ILM-C10, the dispersion polymerization of ILMs led to PIL nanoparticles. The average size of all nanoparticles is very small, in the range of 20−40 nm (normalized standard deviation: 0.6−0.7), as confirmed by dynamic light scattering (DLS) analysis. Since the size of nanoparticles is far smaller than the wavelength of light, even at a high concentration of 50/L the nanoparticle solutions appear translucent. The absolute dimension as well as the morphology of the PIL nanoparticles was further verified by transmission electron microscopy (TEM) characterization. The average sizes of these nanoparticles were determined to possess a mean diameter of 25−40 nm. Figure 1A is a representative TEM image of poly(ILM-C14) nanoparticles prepared in this procedure. The nanoparticles are $30 \pm 7.7$ nm in diameter, and they are found in a homogeneously distributed manner. The excellent dispersibility can be attributed to two key factors: (1) compared with usual polymer latexes of above 100 nm, the PIL nanoparticles are quite small, which diminishes Hamaker interaction and effects of gravity. (2) PILs are in fact strong polyelectrolytes, thus the electrostatic repulsion contributes to the stability of the nanoparticles dispersion. Figure 1B is an enlarged view, which depicts the spherical or quasi-spherical shape of the nanoparticles. Since nanoparticles possess a high surface-to-volume ratio, the spherical shape is expected to provide the minimum surface energy. In addition, it can be seen that these nanoparticles are neither simple micelles nor vesicles, otherwise core−shell or hollow morphologies could be observed. When dried in an agglomerated state at room temperature, these nanoparticles maintain their spherical morphology, as confirmed by the scanning electron microscopy (SEM) in Figure 1C.

The very small size (as compared to other latexes made by dispersion polymerization) is related to the powerful stabilizing capability of the imidazolium-based ILMs. Texter et al. have demonstrated that an ionic liquid surfmer (also an ILM) in which

**Table 1. Characterization of Poly(ionic liquid) Latexes Prepared by Dispersion Polymerization of Ionic Liquid Monomers in Aqueous Solution at a Monomer Concentration of 50 g/L at 70°C**

| entry | monomer type[a] | PIL structures | solution state | particle size by DLS/nm[b] | particle size by TEM/nm[c] |
|---|---|---|---|---|---|
| 1 | ILM-C8 | cylinders + irregular particles | turbid + 60% solid | 2400 | |
| 2 | ILM-C10 | cylinders + spherical particles | turbid + 30% solid | 160 | |
| 3 | ILM-C12 | nanoparticles | translucent | 20 | 25 |
| 4 | ILM-C14 | nanoparticles | translucent | 28 | 35 |
| 5 | ILM-C16 | nanoparticles | translucent | 32 | 31 |
| 6 | ILM-C18 | nanoparticles | translucent | 25 | 37 |
| 7 | ILM-C14/C | nanoparticles | translucent | 25 | 30 |
| 8 | ILM-C16/C | nanoparticles | translucent | 24 | 26 |
| 9 | ILM-C18/C | nanoparticles | translucent | 22 | 34 |

[a] ILM-C14/C, ILM-C16/C, and ILM-C18/C (entries 7−9) represent ionic liquid monomers in the presence of 10 mol % divinylimidazolium cross-linker. [b] Volume-averaged values. [c] Numbers are given when products contain a single population of nanoparticles.

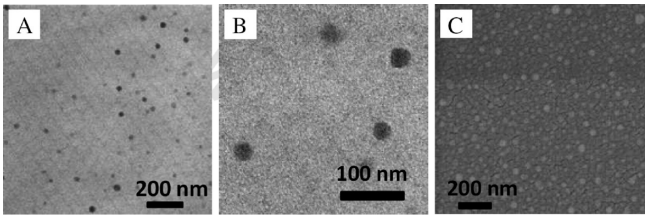


**Figure 1.** Representative TEM (A and B) and SEM (C) images of poly(ILM-C14) nanoparticles, prepared from the dispersion polymerizations of ILM-C14 in water at 70 °C.

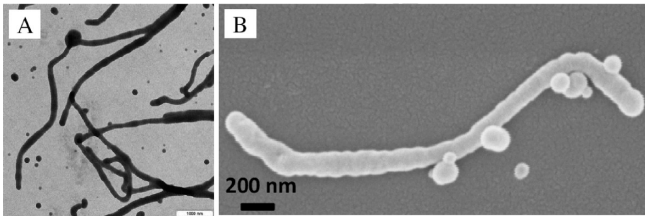


**Figure 2.** Representative TEM (A) and SEM (B) images of poly(ILM-C10) spherical particles and cylinders prepared from the dispersion polymerizations of ILM-C10 in water at 70 °C.

an imidazolium cation and a methacrylate group were bridged by a long alkyl chain that has been copolymerized with methyl methacrylate (MMA) could produce poly(methyl methacrylate)-poly(ionic liquid) (PMMA−PIL) latex with a diameter of ~30 nm.[24]

Solubility test shows that these PIL polymers when dried are insoluble in water, in agreement with previous reports.[21] It implies that the formed nanoparticles in aqueous dispersion have preferentially self-organized that the hydrophilic imidazolium bromide moieties do form the surface. The inner structure of PIL nanoparticles is related to the inherent character of ILMs, which bear a very hydrophilic ion liquid head (ionic pair of an imidazolium cation and a Br anion), and a long hydrophobic alkyl tail that may crystallize. It is true that under the present polymerization conditions the amphiphilic monomers formed micelles,[37,38] with the alkyl chains building up the core and the vinylimidazolium moieties pointing out into water. However, the PIL nanoparticles are no more simple micelles of core−shell structures, because their size (20−40 nm) is far beyond that of a micelle built up from these ILMs; thus some more organized substructure rather than a single micellar structure must exist within these nanoparticles. On the basis of the results of light scattering measurements, Zana et al. have proven that the polymerization of amphiphilic monomers *n*-alkyldimethyl-(vinylbenzyl)ammonium chlorides (alkyl chain = C8, C10, C12 and C16) in water did not follow the mechanism of a topochemical polymerization that would form small "polysoap" micelle structures.[46] They further concluded by time-resolved fluorescence quenching experiments the existence of successive hydrophobic microdomains that were closely located near each other in aqueous dispersions of the polymers. Independently Bremilla et al. reported in the same time that poly(ILM-C16) when dispersed in aqueous media formed hydrophobic microdomains, which had a more compact and tighter structure when compared to the micelles of 3-*n*-hexadecyl-1-methylimidazolium bromide.[42] Later the same group employed cryogenic TEM to image for the first time the presence of close-packed hydrophobic microdomains of 4 ± 1 nm in size that formed when dispersing poly(1-hexdecylvinyl-3-vinylpyridinium bromide) (an analogue polymer of poly(ILM-C16)) from ethanol into water.[35] On the basis of these considerations, the nanoparticles prepared here are most likely setup in organized mesophases made up from separated nanodomains of ionic liquid moieties and the long alkyl chains, with the former more favorably located on the outer surface for stabilizing the entire nanoparticle. Indeed, those well organized local structures of ILs have recently been quantified by silica nanocasting.[47,48]

Although a complete picture of the nanoparticle formation mechanism is not generated yet, it can be assumed that at the initial stage of the polymerization radicals generated from the decomposing of the initiator VA86 in aqueous media were added to the ILMs that existed in a micelle state. The relative lower propagating rate compared to the rapid monomer exchange of ILMs between micelles, allowed the polymerization to proceed with more monomers diffused inside the micelles.[49] This is responsible for the large size of the as-synthesized nanoparticles beyond the initial micellar dimensions. While the polymer chains continually grew within the micelles during the polymerization, polymers started to alter the conformation to overcome the sterical tension and phase separation occurred. This forced a morphological transition from micellar structures to more complex polymer aggregates that have inner structures of hydrophobic multidomains. Eventually when all ILMs were consumed, the polymerization ended up with PIL nanoparticles, made up from phase-separated polymeric aggregates on the nanometer scale.

A change of inner nanostructure with decreasing tail length can drive the morphological transition of PILs dispersions from nanoparticles to more extended structures. This takes place when the alkyl chain length in the employed ILMs decreases from C12 to C10 and C8. The dispersion polymerization of ILM-C8 and C10 produced turbid solutions with 30 and 60 wt % precipitates, respectively. Instead of a single population, a mixture of cylinders and particles were identified in the turbid solutions. DLS measurements revealed that the poly(ILM-C10) dispersion has an apparent hydrodynamic size of 160 nm, and poly(ILM-C8) of 2400 nm. Figure 2A displays a representative TEM image of PILs obtained by dispersion polymerization of ILM-C10 in aqueous solution. Cylinders irregular in length and with an average diameter of 160 nm were observed coexisting with spherical particles of 150 nm in diameter. The SEM image in Figure 2B depicts the surface morphology of a cylinder with surrounding

particles. The cylinders are obviously composed of rather narrowly distributed primary spherical particles, i.e., it is a directional colloidal instability driving the aggregation toward organized larger structures. In the case of poly(ILM-C8), irregular particles and cylinders of ca. 200 nm in diameter and length up to several hundreds of micrometers were observed. These PIL cylindrical structures are potentially of great interest for materials scientists to build up one-dimensional anisotropic functional materials.

PIL nanoparticles prepared from homopolymerization of ILMs are expected to have potential applications as coatings, binders, dispersants, and more. For example, PMMA−PIL nanolatexes with imidazolium moieties on surface, have been successfully used to stabilize single-wall carbon nanotubes in water up to a concentration of 0.5 wt %.[36] Very recently, using the same nanolatexes to stabilize tungsten carbide nanoparticles in aqueous solution has been reported as well.[50] Besides, PIL nanolatexes might be of special interest as sorbents since they possess very high surface area due to a smaller size compared to conventional polymer latexes. In some cases in which organic solvents are involved, care should be taken that the organic solvent might dissolve the PIL nanoparticles. The solubility of these PILs in dioxane, ethanol, DMF, chloroform, and toluene are summarized in the Supporting Information. Chloroform is in general a good solvent for all of these PILs. Ethanol and DMF can dissolve the PILs with limited alkyl chain length up to decyl (C10) and tetradecyl (C14), respectively. Dioxane and toluene are nonsolvents for all PILs and toluene can swell PILs with hexadecyl and octadecyl chains to a certain extent. Therefore, in contact with organic solvents such as chloroform, ethanol, and DMF, PIL nanoparticles might be dissolved into individual macromolecules. To prove this speculation, a controlled experiment was carried out to dialyze poly(ILM-C14) nanoparticles in aqueous solution against DMF. TEM characterization of the PIL in DMF failed to detect the existence of nanoparticles. A similar observation was made when PIL nanoparticle solution was directly added into excessive DMF solvent. To keep particles intact even under those conditions, further efforts were made. An approach which has been widely adopted in polymer chemistry is to chemically cross-link the nanoparticles. In this context, we performed the dispersion polymerization of ILMs in aqueous solutions in the presence of 10 mol % (with respect to ILMs) of the cross-linking agent 1,4-butanediyl-3,3′-bis-l-vinylimidazoliurn dibromide (BVD). The results are presented in Table 1 (entries 7−9). Structurally this divinylimidazolium cross-linker is a conjugation of two vinylimidazolium bromide units via a butyl linker, thus it has a high chemical similarity to ILMs. This minimizes the structural inhomogeneity in the nanoparticle entities and actually maintains the PIL nature of the nanoparticles. The obtained dispersion was translucent and stable, very similar to the noncross-linked systems. DLS measurements show that the average size of the cross-linked nanoparticles was 3−8 nm smaller than the noncrosslinked ones. In line with this, TEM characterization of these nanoparticles indicates a decrease in size of 3−5 nm when nanoparticles were prepared by the cross-linking process. TEM images (Figure 3, parts Aand B) display poly(ILM-C14/C) nanoparticles obtained in this procedure. It was observed that cross-linked poly(ILM-C14/C) nanoparticles are 30 ± 4 nm in diameter, 14% smaller than the noncross-linked ones (35 ± 7 nm). The integrity of these cross-linked nanoparticles was tested in DMF. After dialysis of the aqueous dispersion of the cross-linked PIL nanoparticles against DMF, these nanoparticles were indeed refound, as proven by the TEM characterization (Figure 3, parts C and D). The size slightly increases to 40 ± 5 nm indicating a certain degree of swelling of the PIL nanoparticles. Hence, cross-linking was successful.

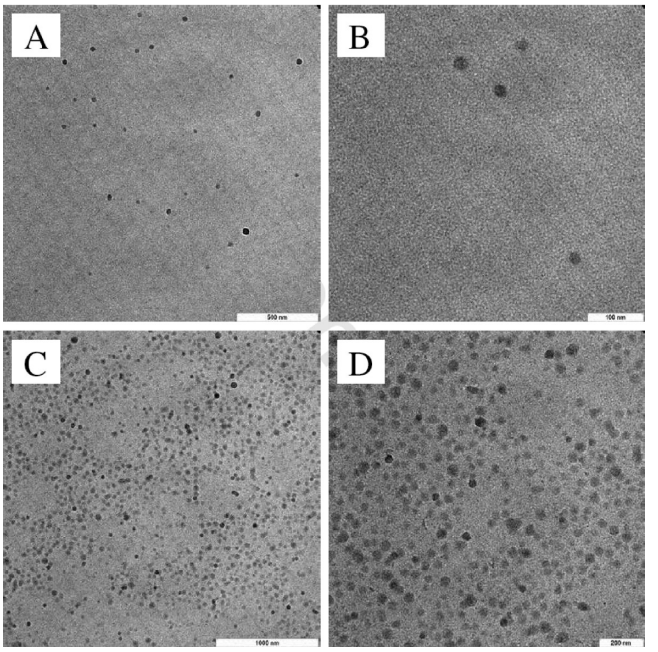


**Figure 3.** TEM images of cross-linked poly(ILM-C14/C) nanoparticles in water (A and B) and in DMF after dialysis (C and D). The scale bars are 500 (in A), 100 (in B), 1000 (in C), and 200 nm (in D).

Nonpolar organic solvents, such as toluene, unfortunately do not disperse the as-synthesized cross-linked PIL nanoparticles, since the surface of these nanoparticles is obviously still highly hydrophilic, full of ion pairs of imidazolium cation and bromide anion. To transform the cross-linked PIL nanoparticles even into nonpolar organic solvents relies on a typical IL effect. The chemistry of ionic liquid has taught us that anions are usually more dominant than the cations in determining the hydrophilicity of ILs. Lithium bis(trifluoromethylsulfonyl)imide ($LiTf_2N$) has been widely used to turn hydrophilic ILs into hydrophobic ones by anion exchange. Therefore, an anion exchange process was performed in the aqueous solution of cross-linked PIL nanoparticles. $LiTf_2N$ was added dropwise into an aqueous solution of cross-linked poly(ILM-C14/C) nanoparticles. The solution became turbid, followed by a phase separation, leaving a clear aqueous supernatant and a white precipitate at the bottom (see Supporting Information). The precipitation was caused because the hydrophobic $Tf_2N$ replaced the bromine, according to ordinary solubility product rules, and varied the nanoparticle surface from being hydrophilic to being hydrophobic. During this process, the nanoparticles were no longer soluble in aqueous solution, agglomerated and sedimented. After the separation of the precipitate and washing with methanol, the precipitate was redispersed into toluene by ultrasonication and gentle heating. The dispersion stayed transparent and stable. TEM characterization (Figure 4) clearly shows that the nanoparticles kept well dispersed as that before anion exchange. The spherical shape actually remained, although a tiny portion of elliptical nanoparticles caused by fusion of two primary nanoparticles were observed. A statistic calculation suggested that the size of these hydrophobic nanoparticles increase slightly from 30 ± 4 to 38 ± 7 nm. This is perhaps caused by a slightly swollen state of nanoparticles in toluene. Another contribution may arise from the anion exchange with the larger sized $Tf_2N$ anions.

Apart from the sensitivity toward solvents, the waterborne PIL nanoparticles were found responsive to the ionic strength in aqueous solution. Independent of the alkyl chain length as well as the cross-linking state, the aqueous solution of nanoparticles became instable when salt was added. This is very typical for

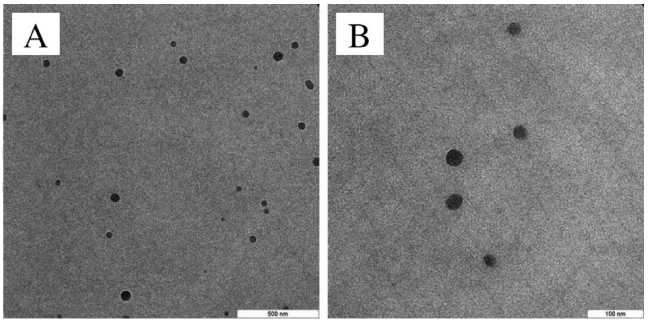


**Figure 4.** TEM images of cross-linked poly(ILM-C14/C) nanoparticles in toluene after anion exchange. The scale bars are 500 nm in A and 100 nm in B.

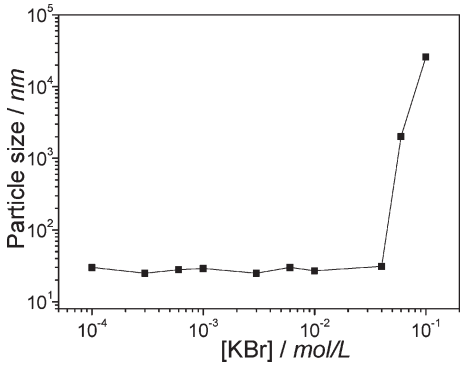


**Figure 5.** Plot of the size of cross-linked (ILM-C14/C) nanoparticles vs the concentration of KBr in aqueous solution. The concentration of PIL nanoparticles is ~10 g/L.

polymer latexes. Cross-linked poly(ILM-C14/C) nanoparticles were chosen as a model system to quantitatively demonstrate the effect of ionic strength. In general, PIL are strong and permanent polyelectrolytes, but addition of salt will screen the electrostatic interaction and compress the electric double layer of nanoparticles in water. A sufficiently high salt concentration will give rise to coagulation of nanoparticles. Figure 5 illustrates the size evolution of cross-linked poly(ILM-C14/C) nanoparticles via the addition of monovalent KBr salt. Up to a salt concentration of 0.03 mol/L, the PIL nanoparticles remained well-dispersed as individual nanoparticles of 30 ± 5 nm. This tolerance enables a wide range of ionic initiators to be used in the dispersion polymerization of ILMs. For instance, V50 has been tested and offered similar results to VA86. However, above 0.03 nol/L, flocculation started and the solution turned turbid. DLS measurements showed that the particle size reached 2 $\mu$m at a KBr concentration of 0.06 mol/L, and 26 $\mu$m at 0.1 mol/L. In the latter case, macroscopic precipitates formed immediately by the introduction of salt. This observation is somehow contradictive with the findings reported earlier by Texter et al., who synthesized PMMA−PIL nanolatexes (~30 nm) that were colloidally stable in 0.1 M aqueous NaBr solution. To understand this difference between these two PIL latexes, two factors should be considered. (1) The present PIL nanoparticles were prepared by dispersion polymerization of ILMs (with/without a divinylimidazolium cross-linker) in aqueous solution where the ILMs existed in a micelle state, whereas PMMA−PIL nanoparticles were generated by microemulsion polymerization of MMA in the presence of equal-molar ILM comonomers as stabilizer. The ILMs in the latter case formed micelles that were swollen by MMA monomer, leading to an averagely lower density of imidazolium bromide moiety in the as-synthesized nanoparticles. (2) It is obvious that the intrinsic chemical structures of the respective ILMs are significantly different. As for the ILMs studied here, the imidazolium bromide moiety is proximal to the vinyl group and anchor for the hydrophobic alkyl tail rather than being at the end of a tether, thus the charges are very close to the backbone. Differently, an acrylate group was distal to the imidazolium bromide moiety in the case of PMMA−PIL nanoparticles, providing more space between the charges and the backbone. We suppose that the above-mentioned factors (independent, synergistic or antagonistic) might alter the density of imidazolium bromide moieties on the nanoparticle surface and consequently vary the sensitivity to added salts. The poly(ILM-C14/C) nanoparticles kept stable up to a [$Br^-$] concentration of 0.03 mol/L, much lower than 0.1 mol/L for PMMA−PIL nanoparticles, indicating their surface was composed of a much denser layer of imidazolium bromide moieties.

## Conclusions

In conclusion, a facile synthetic route to vinylimidazolium-typed poly(ionic liquid) (PIL) latexes and nanoparticles was delineated via dispersion polymerization of ionic liquid monomers in aqueous solutions at 70 °C without any dispersant. When ionic liquid monomers with sufficiently long alkyl chains (≥C12) were used, PILs nanoparticles of 20−40 nm in diameter were found, which were self-stabilizing in aqueous solution. Cross-linked PIL nanoparticles were prepared in the same procedure in the presence of 10 mol % of divinylimidazolium-based cross-linker. They showed improved stability in organic polar solvent, such as DMF. *Via* anion exchange with lithium bis(trifluoromethylsulfonyl)imide, the cross-linked nanoparticles could be successfully dispersed in organic nonpolar solvents, such as toluene. This dispersion polymerization method requires no dispersing agent or other formulation aids and thereby enables the large scale synthesis of pure PIL nanoparticles that can be dispersed in both aqueous and organic solvents. The application spectrum of this novel type of organic nanoparticles ranges from coatings and binders to dispersants or colloidal templates for unusual nanostructure synthesis.

**Acknowledgment.** J.Y. would like to thank the Max Planck Society for financial support, Dr. K. Tauer for providing the VA86 initiator and helpful discussions, Dr. Z. Schnepp for SEM measurements, and Dr. J. Weber for his assistance in the DSC measurements.

**Supporting Information Available:** Photographs of poly(ILM-C14/C) nanoparticle solutions without and with the addition of KBr and $LiTf_2N$ salts and a table showing the results for the solubility test of PILs in water, dioxane, ethanol, DMF, toluene, and chloroform. This material is available free of charge via the Internet at http://pubs.acs.org.

## References and Notes

(1) Armand, M.; Endres, F.; MacFarlane, D. R.; Ohno, H.; Scrosati, B. *Nat. Mater.* **2009**, *8*, 621–629.
(2) Plechkova, N. V.; Seddon, K. R. *Chem. Soc. Rev.* **2008**, *37*, 123–150.
(3) Ranke, J.; Stolte, S.; Störmann, R.; Arning, J.; Jastorff, B. *Chem. Rev.* **2007**, *107*, 2183–2206.
(4) Wasserscheid, P. *Nature* **2006**, *439*, 797–797.
(5) Antonietti, M.; Smarsly, B.; Zhou, Y. *Ionic Liq. Synth.* **2008**, *2*, 609−617.
(6) Antonietti, M.; Kuang, D.; Smarsly, B.; Zhou, Y. *Angew. Chem., Int. Ed.* **2004**, *43*, 4988–4992.
(7) Wang, T.; Kaper, H.; Antonietti, M.; Smarsly, B. *Langmuir* **2007**, *23*, 1489–1495.
(8) Frank, H.; Ziener, U.; Landfester, K. *Macromolecules* **2009**, *42*, 7846–7853.

(9) Green, O.; Grubjesic, S.; Lee, S.; Firestone, M. A. *Polym. Rev.* **2009**, *49*, 339–360.
(10) Lu, J.; Yan, F.; Texter, J. *Prog. Polym. Sci.* **2009**, *34*, 431–448.
(11) Williams, S. R.; Long, T. E. *Prog. Polym. Sci.* **2009**, *34*, 762–782.
(12) Green, M. D.; Long, T. E. *Polym. Rev.* **2009**, *49*, 291–314.
(13) Anderson, E. B.; Long, T. E. *Polymer* **2010**, *51*, 2447–2454.
(14) Yuan, J.; Giordano, C.; Antonietti, M. *Chem. Mater.* **2010**, *22*, 5003–5012.
(15) Marcilla, R.; Ochoteco, E.; Pozo-Gonzalo, C.; Grande, H.; Pomposo, J. A.; Mecerreyes, D. *Macromol. Rapid Commun.* **2005**, *26*, 1122–1126.
(16) Marcilla, R.; Curri, M.; Cozzoli, P.; Martínez, M.; Loinaz, I.; Grande, H.; Pomposo, J.; Mecerreyes, D. *Small* **2006**, *2*, 507–512.
(17) Marcilla, R.; Alberto Blazquez, J.; Rodriguez, J.; Pomposo, J. A.; Mecerreyes, D. *J. Polym. Sci., Part A: Polym. Chem.* **2004**, *42*, 208–212.
(18) Ohno, H. *Macromol. Symp.* **2007**, *249*−*250*, 551–556.
(19) Ohno, H.; Yoshizawa, M.; Ogihara, W. *Electrochim. Acta* **2004**, *50*, 255–261.
(20) Yan, F.; Texter, J. *Angew. Chem. Inter. Ed.* **2007**, *119*, 2492–2495.
(21) Salamone, J. C.; Israel, S. C.; Taylor, P.; Snider, B. *Polymer* **1973**, *14*, 639–44.
(22) Amajjahe, S.; Ritter, H. *Macromolecules* **2008**, *41*, 716–718.
(23) Jazkewitsch, O.; Ritter, H. *Macromol. Rapid Commun.* **2009**, *30*, 1554–1558.
(24) Yan, F.; Texter, J. *Chem. Commun.* **2006**, 2696–2698.
(25) Mori, H.; Yahagi, M.; Endo, T. *Macromolecules* **2009**, *42*, 8082–8092.
(26) Vijayakrishna, K.; Jewrajka, S. K.; Ruiz, A.; Marcilla, R.; Pomposo, J. A.; Mecerreyes, D.; Taton, D.; Gnanou, Y. *Macromolecules* **2008**, *41*, 6299–6308.
(27) Ding, S.; Tang, H.; Radosz, M.; Shen, Y. *J. Polym. Sci., Part A: Polym. Chem.* **2004**, *42*, 5794–5801.
(28) Tang, H.; Tang, J.; Ding, S.; Radosz, M.; Shen, Y. *J. Polym. Sci., Part A: Polym. Chem.* **2005**, *43*, 1432–1443.
(29) Yang, J.; Sun, W.; Lin, W.; Shen, Z. *J. Polym. Sci., Part A: Polym. Chem.* **2008**, *46*, 5123–5132.
(30) Yuan, J.; Schlaad, H.; Giordano, C.; Antonietti, M. *Eur. Polym. J.* **2011**, doi:10.1016/j.eurpolymj.2010.09.030 (in press).
(31) Lee, S.; Becht, G. A.; Lee, B.; Burns, C. T.; Firestone, M. A. *Adv. Funct. Mater.* **2010**, *20*, 2063–2070.
(32) Burns, C. T.; Lee, S.; Seifert, S.; Firestone, M. A. *Polym. Adv. Technol.* **2008**, *19*, 1369–1382.
(33) Hsieh, Y.-N.; Kuei, C.-H.; Chou, Y.-K.; Liu, C.-C.; Leu, K.-L.; Yang, T.-H.; Wang, M.-Y.; Ho, W.-Y. *Tetrahedron Lett.* **2010**, *51*, 3666–3669.
(34) Vygodskii, Y. S.; Shaplov, A. S.; Lozinskaya, E. I.; Lyssenko, K. A.; Golovanov, D. G.; Malyshkina, I. A.; Gavrilova, N. D.; Buchmeiser, M. R. *Macromol. Chem. Phys.* **2008**, *209*, 40–51.
(35) Benjelloun, A.; Brembilla, A.; Lochon, P.; Adrian, M.; Ghanbaja, J. *Langmuir* **1997**, *13*, 5770–5773.
(36) Antonietti, M.; Shen, Y.; Nakanishi, T.; Manuelian, M.; Campbell, R.; Gwee, L.; Elabd, Y. A.; Tambe, N.; Crombez, R.; Texter, J. *ACS Appl. Mater. Interface* **2010**, *2*, 649–653.
(37) Salamone, J. C.; Taylor, P.; Snider, B.; Israel, S. C. *J. Polym. Sci.: Polym. Chem. Ed.* **1975**, *13*, 161–170.
(38) Salamone, J. C.; Israel, S. C.; Taylor, P.; Snider, B. *J. Polym. Sci.: Polym. Symp.* **1974**, *45*, 65–73.
(39) Petrak, K.; Degen, I.; Beynon, P. *J. Polym. Sci.: Polym. Chem. Ed.* **1982**, *20*, 783–793.
(40) Tribet, C.; Gaboriaud, R.; Gareil, P. *J. Chromatogr. A* **1992**, *608*, 131–141.
(41) Paleos, C. M.; Voliotis, S.; Margomenou-Leonidopoulou, G.; Dais, P. *J. Polym. Sci.: Polym. Chem. Ed.* **1980**, *18*, 3463–3468.
(42) Damas, C.; Brembilla, A.; Baros, F.; Viriot, M.-L.; Lochon, P. *Eur. Polym. J.* **1994**, *30*, 1215–1222.
(43) Laschewsky, A. In *Polysoaps/Stabilizers/Nitrogen-15 NMR*; Springer: Berlin and Heidelberg, Germany, 1995; Vol. *124*, pp 1−86.
(44) Benjelloun, A.; Damas, C.; Brembilla, A.; Lochon, P. *Polym. Bull.* **1994**, *33*, 513–520.
(45) Leddet, C.; Fischer, A.; Brembilla, A.; Lochon, P. *Polym. Bull.* **2001**, *46*, 75–82.
(46) Cochin, D.; Candau, F.; Zana, R. *Macromolecules* **1993**, *26*, 5755–5764.
(47) Zhou, Y.; Antonietti, M. *Chem. Mater.* **2003**, *16*, 544–550.
(48) Zhou, Y.; Schattka, J. H.; Antonietti, M. *Nano Lett.* **2004**, *4*, 477–481.
(49) Hamid, S. M.; Sherrington, D. C. *Polymer* **1987**, *28*, 332–339.
(50) Giordano, C.; Yang, W.; Lindemann, A.; Crombez, R.; Texter, J. *Colloids Surf. A: Physicochem. Eng. Aspects* **2011**, *374* 84–87.